Spatial molecular layer deposition of polyamide thin films on flexible polymer substrates using a rotating cylinder reactor

Daniel J. Higgs, Jaime W. DuMont, and Kashish Sharma
Department of Chemistry and Biochemistry, University of Colorado, Boulder, Colorado 80309

Steven M. George[a)]
Department of Chemistry and Biochemistry, University of Colorado, Boulder, Colorado 80309
and Department of Mechanical Engineering, University of Colorado, Boulder, Colorado 80309

(Received 10 September 2017; accepted 13 November 2017; published 19 December 2017)

Polyamide thin films were rapidly grown using spatial molecular layer deposition (MLD) in a rotating cylinder reactor. The polyamide MLD films were coated on flexible metalized polyethylene terephthalate substrates using sequential exposures of trimesoyl chloride (TMC) and m-phenylenediamine (mPD). The rotating cylinder reactor was housed in a custom oven enclosure that maintained a constant temperature of 115 °C. One MLD cycle (TMC/mPD) was performed per rotation of the cylinder. Polyamide growth rates of 4.5 Å/cycle or 90 Å/min were observed at a slow rotation speed of 20 revolutions per minute (RPM) at a substrate speed of 0.33 m/s. Growth rates of 2.27 Å/cycle or 477 Å/min were measured at higher rotation speeds of 210 RPM at substrate speeds of 3.5 m/s. The polyamide film thicknesses were uniform over the substrate widths as large as ~16.5 cm. The polyamide MLD surface chemistry was also self-limiting. Constant polyamide growth rate per cycle was measured at larger TMC and mPD exposures. In addition, infrared analysis and thermal annealing studies confirmed the chemical identity of the polyamide films. With four MLD cycles per rotation of the rotating cylinder, spatial MLD should be able to obtain polymer growth rates of >1900 Å/min at a rotation speed of 210 RPM. These rapid growth rates are much higher than the growth rates that can be obtained in temporal MLD reactors. The spatial MLD of polyamide films has many possible applications including the deposition of ultrathin reverse osmosis membranes for water desalination. *Published by the AVS.*
https://doi.org/10.1116/1.5004041

I. INTRODUCTION

Molecular layer deposition (MLD) is closely related to atomic layer deposition (ALD).[1,2] Both ALD and MLD are based on sequential, self-limiting, gas-phase surface reactions that produce highly conformal films with atomic-level thickness control.[3] ALD typically deposits atoms during each sequential set of surface reactions and leads to the growth of inorganic films.[4] MLD is distinguished from ALD because a molecular fragment is deposited during one or more of the surface reactions.[3] MLD can produce all-organic films or hybrid organic–inorganic films.[2,3,5]

Good candidates for MLD are organic polymers that can be deposited using condensation reactions between two reactants.[5,6] The MLD process involves the sequential, self-limiting reactions of the two reactants to grow the organic polymer.[3] These condensation reactions can occur using gas phase precursors without the need of solvents. Various organic polymers, including polyamides,[6,7] polyimides,[8] polyureas,[9] and polyurethanes,[10] have all been deposited by MLD.

Hybrid organic–inorganic polymer films can also be grown using MLD techniques.[2,5] These hybrid organic–inorganic polymer films are usually deposited using one organic precursor with two chemical functional groups and one inorganic precursor with multiple functional groups. One hybrid organic–inorganic polymer film is alucone (aluminum alkoxide) that was first grown using $Al(CH_3)_3$ [trimethylaluminum (TMA)] and ethylene glycol.[11] Other hybrid organic–inorganic metal alkoxide (metalcone) polymer films include the zincones,[12,13] zircones,[14] titanicones,[15] and hafnicones.[16] A wide range of other hybrid organic–inorganic films have also been deposited using MLD techniques.[2,5]

ALD can employ sequential surface reactions where the reactants are separated in time. This type of ALD is known as "temporal" ALD.[17] ALD can also be performed by separating the reactants in space rather than in time. This type of ALD is known as "spatial" ALD.[17] For spatial ALD, the substrate moves relative to separated zones of constantly flowing reactants, inert gas and often pumping.[17] This approach enables much faster growth rates that are governed primarily by substrate translation speeds rather than the purge times of temporal ALD.

Spatial ALD is also compatible with roll-to-roll (R2R) processing of flexible polymer or metal foil.[18–20] The flexible substrate can unwind from the initial roller, move under a gas source head to receive the sequential exposures of reactants, and then rewind on the final roller. R2R spatial ALD will enable many industrial applications of ALD. Possible application areas are ALD coatings as gas diffusion barriers on polymers[21,22] or protective coatings on Li ion battery electrodes.[23,24]

Our previous work has concentrated on the development of a versatile rotating cylinder reactor for spatial ALD.[25,26]

[a)]Electronic mail: Steven.George@Colorado.Edu

This rotating cylinder reactor design is modular and easily allows the reactant, purging and pumping locations to be adjusted for optimum spatial ALD. We have demonstrated Al_2O_3 ALD and ZnO ALD on flexible polyethylene terephthalate (PET) substrates in the rotating cylinder reactor.[25,26] We have also performed ZnO ALD on model flexible anodic aluminum oxide membranes.[26] In addition, Al_2O_3 ALD has been employed to coat flexible Li ion battery electrodes in the rotating cylinder reactor.[26]

Although there have been many advances in spatial ALD,[27–30] there have been no reports of spatial MLD. One of the difficulties of spatial MLD is the typically low vapor pressure of the organic reactants. Low vapor pressures will limit the mass transport of the organic reactants and prevent the MLD surface reactions from reaching completion in a limited time. Low vapor pressures also lead to condensation of the organic reactant at cold locations in the reactor that limit mass transport and can lead to chemical vapor deposition (CVD). The source temperatures of organic reactants can be raised to increase their vapor pressure. However, organic reactants are also thermally fragile and must be kept below their decomposition temperatures.

Many of the problems of using low vapor pressure organic reactants can be avoided by performing MLD in an isothermal environment. For this demonstration of spatial MLD using a rotating cylinder reactor, the rotating cylinder reactor, gas lines and precursor sources were all placed inside an isothermal enclosure. This isothermal design significantly improved the ability to perform MLD by eliminating any cold locations. Using this new isothermal enclosure, polyamide MLD films were deposited using sequential exposures of trimesoyl chloride (TMC) and m-phenylenediamine (mPD). The growth of this polyamide film was used to characterize the spatial MLD rotating cylinder reactor and the dependence of polyamide film growth on reaction conditions.

The reaction of TMC and mPD to form a polyamide film is frequently used to fabricate polyamide films for reverse osmosis membranes for water desalination.[31,32] Polyamide films are stable and chemically resistant to the chemical environment during water desalination. Polyamide films can also be formed with TMC and mPD using interfacial polymerization methods.[33–35] For thickness control of the polyamide film, previous work has employed liquid-phase layer-by-layer (LbL) deposition using the TMC and mPD reactants.[36,37] Gas phase MLD can obtain better thickness control and can be performed much faster than liquid-phase layer-by-layer deposition. The gas phase MLD approach also avoids the solvents, cleaning steps, and drying steps used in the liquid-phase approach.

II. EXPERIMENT

A. Polyamide reaction chemistry and flexible substrates

This demonstration of spatial MLD utilized a polyamide condensation reaction.[2,5,7] In this reaction, the chloro-acid group of one monomer reacts with the amine group of the other monomer to produce an amide linkage and HCl as a reaction side product. Figure 1 shows the reaction of TMC and mPD used to deposit the polyamide MLD film in this study. The trifunctionality of the TMC precursor allows the reaction of the acid-chloride groups with the amine groups on the bifunctional m-phenylenediamine to produce amide linkages and form a network polymer. Network polymers are not possible with only bifunctional precursors.

To perform the polyamide MLD, two custom-made gold-coated 316L steel containers were filled separately with TMC (98%, Sigma Aldrich) and mPD (99%, Sigma Aldrich). These precursor containers were connected to the rotating cylinder reactor using a pneumatically actuated valve (Swagelok high-pressure, pneumatically actuated bellows-sealed, HB series, $C_v = 0.3$) and a manually adjustable conductance-limiting valve (Swagelok, bellows-sealed metering valve, BM series, $C_v \leq 0.3$). The precursors were held at the temperature of the isothermal enclosure.

The polyamide MLD films were deposited on flexible Ti-metalized PET polymer substrates. The reflective metalized PET facilitated analysis of the polyamide MLD film thickness using spectroscopic ellipsometry (SE). Samples of metalized PET (Rowo Coating) were cut from a large roll and taped to the rotatable inner cylinder with Kapton™ tape. The samples were utilized as received without any additional cleaning. The rotatable inner cylinder was heated to 115 °C in the custom oven enclosure described below. The samples were left to degas and thermally equilibrate for a few hours.

B. Rotating cylinder reactor design and oven enclosure

The spatial MLD of the polyamide film was performed in the rotating cylinder reactor. The design of this rotating cylinder reactor has been described previously.[25] Briefly, this spatial MLD reactor uses a rotating inner cylinder with a diameter of 12.5 in. and circumference of 39 in. as the substrate stage. The rotating cylinder can rotate at speeds up to 210 revolutions per minute (RPM). Concentric to the inner cylinder is a fixed outer cylinder with 31 modular slits capped with pumping, dosing, or purging modules or aluminum blanks. The modules can be moved to different

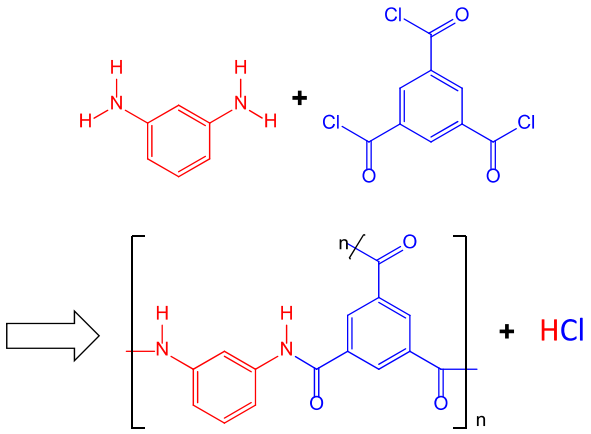

FIG. 1. (Color online) Reaction of TMC and mPD to deposit network polyamide MLD film and HCl.

locations on the outer cylinder to vary reaction conditions to optimize the deposition.

Figure 2 shows a picture of the dosing, pumping, and purging modules that were attached to some of the 31 fixed slit module positions on the outer cylinder. None of the connections to the modules are shown for clarity. There are pumping modules on both sides of the TMC and mPD precursor modules. Three mechanical rotary vane pumps (D8B, Oelerkon Leybold) provided pumping for the reactor and the pumping modules. Aluminum blanks are on the slits between the precursor and pumping modules. There are nitrogen purging modules [100 sccm total, ultra high purity (UHP) N_2] on the outside of the pumping modules. Aluminum blanks are again on the slits between the pumping and purging modules. All other slits are capped with aluminum blanks.

Figure 3 shows a schematic of the gas flow for one dosing, pumping, and purging zone. The precursor molecules travel from the precursor reservoir to the mechanical pump via the substrate. The effect of the low vapor pressure of the organic precursors was minimized by placing the pumping module between the precursor and the nitrogen purge modules. The gap between the rotating inner cylinder and fixed outer cylinder is only 750 l m. Consequently, the precursor molecules have multiple collisions with the substrate surface as they travel to the pump. The small gap allows precursors to fill the gap quickly and leads to efficient utilization of the precursors.

The precursor exposures are reported in terms of the flow coefficient (Cv) of the conductance limiting valve (Swagelok, BMRG) that is between the precursor reservoir and the substrate. The flow coefficient, Cv, is defined by the manufacturer (Swagelok). The flow coefficient is the volume, in US gallons, of water that will flow through a valve at 60 °F over 1 min with a pressure drop of 1 psi across the valve.

This flow coefficient cannot be easily translated to a mass flow rate because the pressure drop across the valve is not known and cannot be easily determined. By increasing the aperture of the variable conductance limiting valve, the flow coefficient will increase according to a calibration curve that correlates the number of turns that the valve is opened to the Cv. The flow coefficient can be assumed to be proportional to the mass flow of molecules through the valve. The flow coefficient is directly related to the exposure of precursor molecules on the surface.

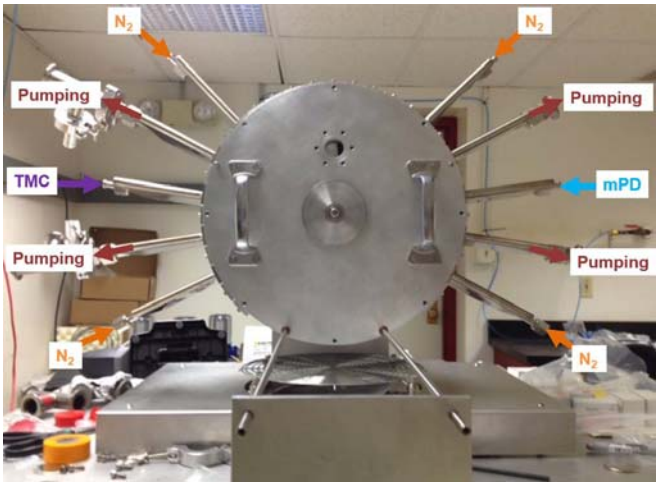

FIG. 2. (Color online) Front of spatial MLD reactor showing modules for precursor dosing, pumping and nitrogen purging. None of the connections to modules are shown for clarity. One TMC/mPD reaction cycle occurs during one rotation of inner cylinder.

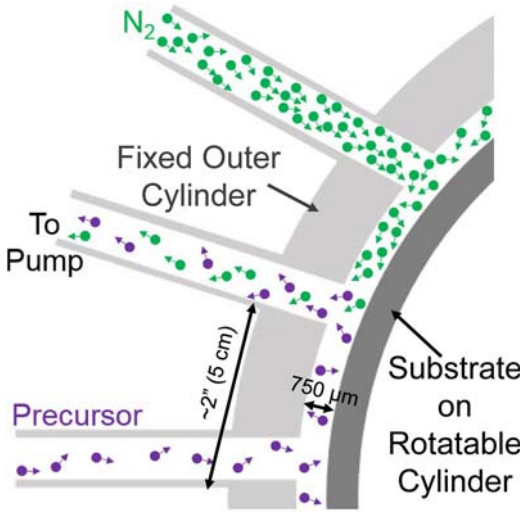

FIG. 3. (Color online) Gas flow of precursor and N_2 molecules for one dosing, pumping, and purging zone on the rotating cylinder reactor.

One difference between this spatial MLD reactor and the previously reported spatial ALD reactor[25] was the operating pressure. The previously reported spatial ALD reactor used 200 sccm of N_2 purge flowing in the four purging modules. In contrast, the spatial MLD reactor in this study used only 100 sccm of N_2 flowing in the four purging modules. This difference in N_2 flow rates, as well as differences in pumping speeds, resulted in a background operating pressure of <1 Torr in the spatial MLD reactor. The background operating pressure of the earlier spatial ALD reactor was $\sim$18 Torr.[25] The lower pressure in the spatial MLD reactor enabled the low vapor pressure precursors to be efficiently delivered to the substrate without resistance from higher N_2 pressures.

To maintain constant temperature, the rotating cylinder reactor, as well as the gas lines and precursor reservoirs, was placed inside a custom oven enclosure. This oven enclosure could be heated to 150 °C and maintained uniform temperatures. The temperature was measured by a K-type thermocouple in the custom oven enclosure. The output from this thermocouple was the input for a proportional–integral–derivative temperature control system. Additional K-type thermocouples residing in the enclosure, in the ambient air, on the outer cylinder or on the precursor sources revealed that the temperature was uniform to within <2 °C. Figure 4(a) shows a computer aided design model of the spatial MLD reactor inside the oven enclosure. The translucent cover shown is, in reality, an opaque, 2 in. thick, custom-made insulation cover (Valin Corporation, CO).

Underneath the insulation cover is a custom extruded aluminum inner frame that supports the weight of the insulation cover. The top four corners of the inner frame are connected

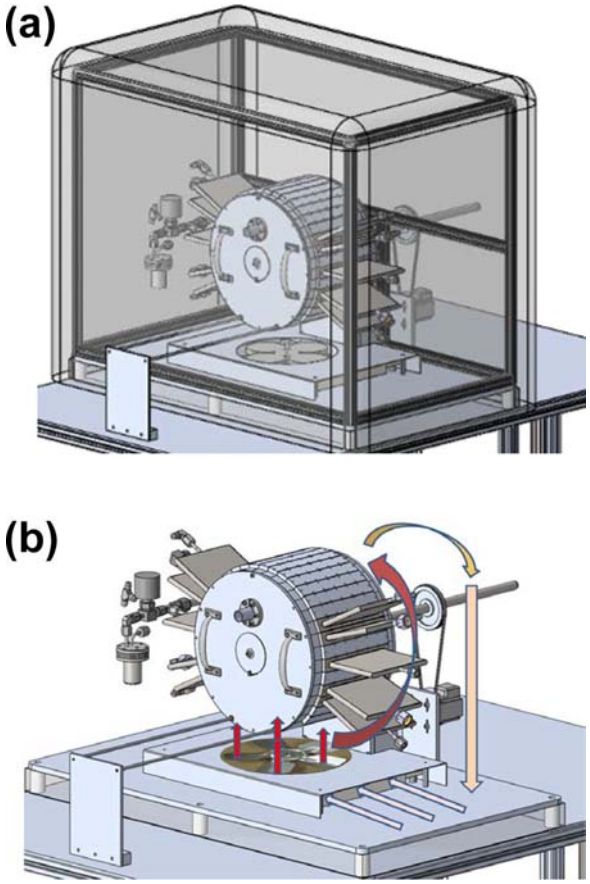

FIG. 4. (Color online) Drawings of spatial MLD reactor. (a) Spatial MLD reactor in a custom oven enclosure. (b) Illustration of air flow in custom oven enclosure with enclosure removed for clarity.

to another frame that sits outside and on top of the insulation cover. This frame is connected to a mechanical winch (not shown) that can lift the frame to provide access to the rotating cylinder reactor.

Figure 4(b) shows the base of the oven and the rotating cylinder reactor. Underneath the rotating cylinder reactor are two finned resistive 750 W heating elements on both sides of a high-speed fan. The fan blade is connected to the fan motor by a shaft that goes down from the fan blade and through the insulation on the bottom of the enclosure. Tubing and wiring for pumping, pneumatic actuation, and capacitance manometers all enter and exit the base of the oven through the insulation on the bottom of the enclosure. The hot air heats the reactor as the air is blown upwards before hitting the top of the insulation cover. The air circulates back down to the base where the air is drawn across the heaters again.

C. Polyamide sample analysis

The resulting MLD films were characterized with a variety of techniques including SE, Fourier transform infrared (FTIR) spectroscopy and x-ray photoelectron spectroscopy (XPS). For the SE and XPS analysis, samples were cut from the MLD-coated metalized-PET samples. The SE measurements were conducted using an M-2000 ellipsometer from J.A. Woollam. The SE results were analyzed using a Cauchy model. The XPS analysis was performed with a PHI 5600 XPS spectrometer using a monochromatized Al Ka x-ray source. Additional micro Raman measurements utilized a Renishaw inVia at 514 nm with a 2400 lines/mm grating.

The FTIR experiments utilized high surface area ZrO_2 nanoparticles (99.5%, US Research Nanomaterials) with an average diameter of 15–20 nm. The large surface area improved the signal-to-noise ratio for the infrared absorption measurements.[38] The ZrO_2 nanoparticles were mechanically pressed into a stainless steel grid support.[39] The sample grids were $2 \times 3\,cm^2$, 50 l m thick, with 100 grid lines per inch. The ZrO_2 nanoparticles in the stainless steel grids were then attached to the inner cylinder of the rotating cylinder reactor with Kapton tape. After the polyamide MLD, the stainless steel grids were removed from the reactor and analyzed in a separate vacuum chamber equipped for transmission FTIR studies.[38]

III. RESULTS AND DISCUSSION

A. Initial Al_2O_3 ALD characterization

Initial tests were conducted to characterize the rotating cylinder reactor. These tests were performed using Al_2O_3 ALD with TMA and O_3 as the reactants at room temperature. In agreement with our earlier results for Al_2O_3 ALD in rotating cylinder reactors,[25] this initial characterization obtained Al_2O_3 ALD films with linear growth rates of 1.0 Å/cycle at 20 RPM. After confirming the successful performance of the reactor with Al_2O_3 ALD, the TMA and O_3 precursors were replaced with TMC and mPD, respectively.

B. Polyamide film growth

Figure 5 displays the thickness of the polyamide MLD film as determined by SE versus the number of spatial MLD cycles. This MLD growth was performed at 20 RPM and 115 °C. Twenty revolutions per minute is equivalent to a substrate speed of 20 m/min and 20 MLD cycles/min with the reactor configured for one MLD cycle per rotation. The precursor exposures were defined by the flow coefficients of the conductance limiting valves at Cv = 0.017 for TMC and Cv = 0.017 for mPD.

The polyamide film growth is linear. Figure 5 shows that the growth rate is ~4.5 Å/cycle. The y-intercept fitted to the data points goes through the origin. This behavior indicates that the polyamide MLD nucleates well on the metalized PET polymer substrates. The thickness of the polyamide film could be controlled by the number of MLD cycles. The thinnest polyamide MLD film tested during these experiments had a thickness of 80 Å.

The 4.5 Å/cycle growth rate is less than the estimated maximum thickness of ~12 Å for one monolayer of TMC reacting with mPD in an orientation perpendicular to the surface.[37] This maximum thickness estimate of ~12 Å is based on bond lengths and trigonometry assuming a planar configuration where an acid chloride group on the TMC reacts with an initial surface hydroxyl group and the central axis of the TMC is oriented perpendicular to the surface. An amine group on the mPD then reacts with one of the

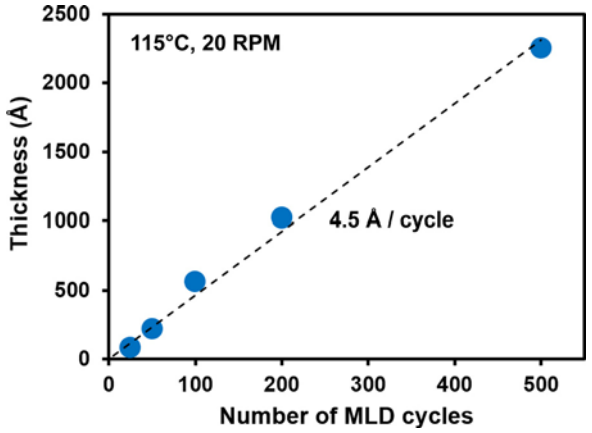

FIG. 5. (Color online) Polyamide MLD film thickness vs number of spatial MLD cycles at 115 °C and 20 RPM with Cv = 0.017 for both TMC and mPD. Linear growth yields growth rate of 4.5 Å/cycle.

remaining acid chloride groups on the TMC and the other remaining amine group on the mPD is oriented perpendicular to the surface.

The maximum thickness estimate of ~12 Å for one monolayer of polyamide MLD is an upper limit. The actual thickness will be less if the TMC and mPD do not produce a planar configuration oriented perpendicular to the surface. Bond rotations could break the planar configuration. The growth direction may also not be perpendicular to the surface. Low rates for polyamide MLD film growth using terephthaloyl chloride and p-phenylenediamine were explained by polymer chains growing approximately parallel to the initial surface like a "tangled pile of spaghetti."[7] Near-edge x-ray absorption fine structure studies of an alkyl-aromatic polyamide film using 1,4-butane diamine and terephthaloyl dichloride as the reactants also revealed that the polymer chains were lying nearly parallel to the surface.[40] The measured polyamide MLD growth rate of 4.5 Å/cycle is intermediate between a polymer chain orientation perpendicular and parallel to the initial substrate.

A growth rate of 8.8 Å/cycle was reported for polyamide growth with TMC and mPD using the LbL liquid phase technique.[37] The measured MLD growth rate of 4.5 Å/cycle is lower than the LbL growth rate of 8.8 Å/cycle. The differences between the MLD growth and the LbL synthesis may result from different reaction conditions existing in the gas phase and the liquid phase. In addition, the LbL synthesis requires solvent rinsing and spin-drying after each reaction step. Incomplete reactant removal could lead to higher growth rates during the subsequent reaction.

Figure 6(a) shows a photograph of a large metalized PET sample coated with 100 cycles of spatial polyamide MLD at 115 °C and 20 RPM. This sample has dimensions of 160 mm in length and 70 mm in width. The precursor exposures were defined by the flow coefficients of the conductance limiting valves at Cv = 0.017 for TMC and Cv = 0.017 for mPD. The sample was placed in the reactor such that the 160 mm length of the sample was centered along the width of the rotating cylinder. The length of this sample was the same length as the long dimension of the dosing slits. The gold color results from optical interference effects. This color is uniform and suggests a conformal polyamide film with low roughness.

Figure 6(b) displays the polyamide thickness as measured by SE at the center from left to right along the 160 mm length of the sample. The thicknesses were identical along the 70 mm width of the sample in the direction of rotation. The polyamide thickness is uniform and increases slightly in thickness towards the edge of the sample. This thickness increase is likely due to a small amount of CVD at the ends of the dosing slits. TMC and mPD precursors that are not pumped by the pumping modules will escape through the gaps at the outside edges of the rotating cylinder. These precursors could react with each other resulting in some CVD.

Figure 7 shows the thickness versus exposure curves for 500 cycles of polyamide MLD at 115 °C and 20 RPM. As the mPD or TMC exposure is increased with the other precursor exposure fixed, the MLD thickness increases until the MLD thickness reaches a limiting thickness. Figure 7(a) shows the polyamide thickness versus mPD flow with the TMC flow fixed at Cv = 0.017 (1/2 turn open). The self-limiting thickness is nearly reached at an mPD flow of Cv = 0.017. The thickness does not increase significantly with larger mPD exposures. Figure 7(b) shows the polyamide thickness versus TMC flow with the mPD flow fixed at Cv = 0.017 (1/2 turn open). A self-limiting thickness is again nearly reached at a TMC flow of 0.017. Much larger TMC flows of ≥0.15 lead to somewhat higher film thicknesses. These higher film thicknesses may be attributed to some additional CVD growth at larger TMC flows.

Figure 8 shows the polyamide thickness and growth rate after 500 cycles of spatial MLD at various rotating cylinder speeds at 115 °C. The precursor exposures were defined by the flow coefficients of the conductance limiting valves at Cv = 0.017 for TMC and Cv = 0.017 for mPD. Polyamide growth rates of 4.5 Å/cycle or 90 Å/min were measured at a

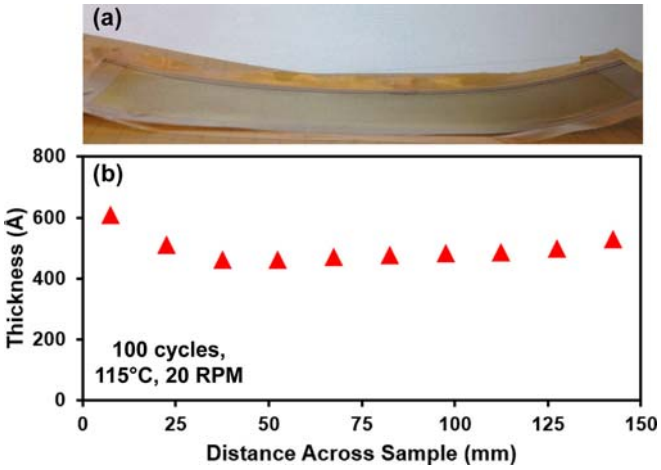

FIG. 6. (Color online) (a) Photo of 160 × 70 mm sheet of metalized PET polymer coated with 100 MLD cycles at 115 °C and 20 RPM with Cv = 0.017 for both TMC and mPD. Gold color indicates uniform thickness across sample. (b) Polyamide MLD film thickness vs distance across sample showing uniform thickness over most of sample.

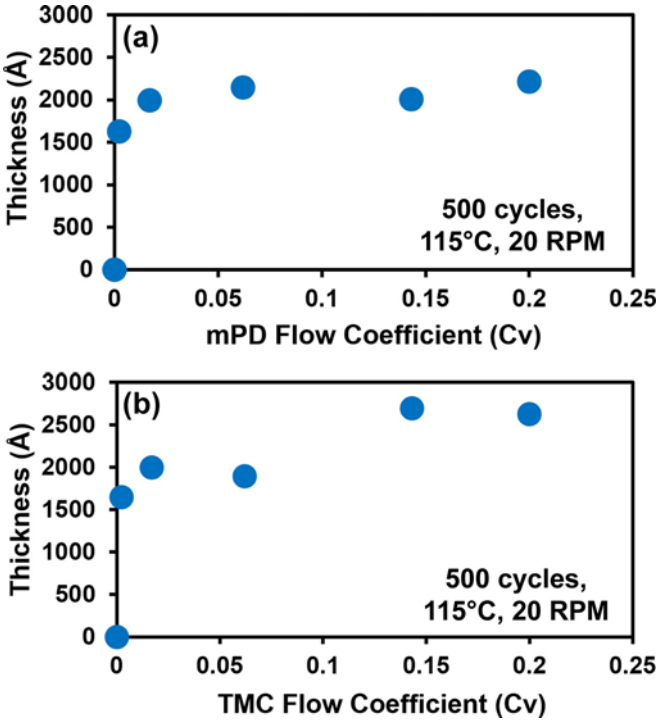

FIG. 7. (Color online) Saturation curves showing self-limiting behavior of (a) mPD reaction with TMC exposure fixed at Cv = 0.017 and (b) TMC reaction with mPD exposure fixed at Cv = 0.017 during polyamide MLD at 115 °C and 20 RPM.

slow rotation speed of 20 RPM. Growth rates of 2.27 Å/cycle or 477 Å/min were observed at higher rotation speeds of 210 RPM. These results were obtained with only 1 MLD cycle per revolution of the rotating cylinder. The current rotating cylinder reactor has enough modules to accommodate 4 MLD cycles per rotation. With four MLD cycles per rotation of the rotating cylinder, growth rates of ~1900 Å/min could be obtained at a rotation speed of 210 RPM.

A decreasing polyamide thickness is produced at the higher rotation speeds. This behavior can be explained by the lower precursor exposure times at the faster rotating cylinder speeds.[26,41] The faster the cylinder rotates, the less time the substrate is in the precursor zone. Faster rotating cylinder rates lead to shorter exposure times for the precursor to react with the substrate. At 210 RPM, the precursors are only exposed to the surface for ~10 ms. This short time is not long enough for the surface reaction to reach completion. Similar behavior was observed earlier for spatial ALD using TMA and ozone.[25]

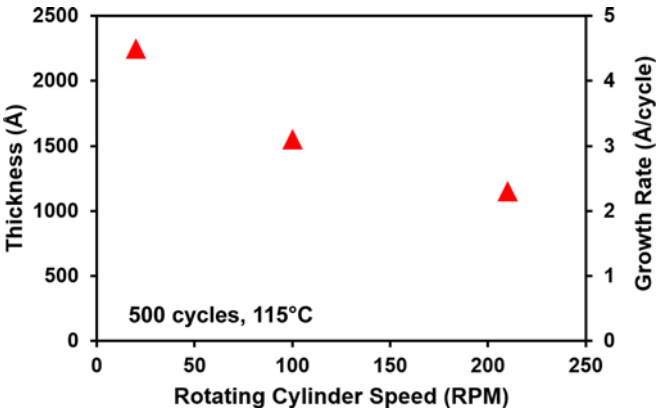

FIG. 8. (Color online) Polyamide MLD film thickness vs rotating cylinder speed for 500 MLD cycles at 115 °C with Cv = 0.017 for both TMC and mPD. Growth rate is 4.5 Å/cycle or 90 Å/min at 20 RPM and 2.27 Å/cycle or 477 Å/min at 210 RPM.

C. Characterization of polyamide films

Figure 9 shows the FTIR spectrum of the network polyamide film grown using 25 MLD cycles of TMC and mPD at 115 °C and 20 RPM on a ZrO_2 nanoparticle substrate. The precursor exposures were defined by the flow coefficients of the conductance limiting valves at Cv = 0.017 for TMC and Cv = 0.017 for mPD. The FTIR spectrum in Fig. 9 is consistent with previously reported FTIR spectra of network polyamide films.[42–44] The repeat units in the polyamide film give rise to characteristic IR absorption bands such as the amide A, amide B, amide I, amide II, and amide III bands.[42–44] The amide IV–VIII bands occur at $<625\,cm^{-1}$ and are not measurable because of the strong absorption from the ZrO_2 nanoparticles at $<800\,cm^{-1}$.

The amide A and amide B bands represent N-H stretching vibrations and are observed in Fig. 9 at 3225 and $3070\,cm^{-1}$, respectively. The amide I band is attributed to the C=O stretching vibrations of the amide group and is monitored at $1665\,cm^{-1}$. The amide II band derives mainly from in plane N-H and C-N stretching vibrations and is detected at $1530\,cm^{-1}$. The amide III band is more complex and results from mixtures of several coordinate displacements. The amide III band is monitored at $\sim1300\,cm^{-1}$. In addition, a peak at $1610\,cm^{-1}$ is detected that is attributed to the C=C vibrational stretching within the aromatic ring structures.

Unreacted -COCl groups may react with water to form -COOH groups when exposed to atmosphere according to the following reaction: $\text{-COCl} + H_2O \rightarrow \text{-COOH} + HCl$. The –COOH groups have a characteristic absorption for the

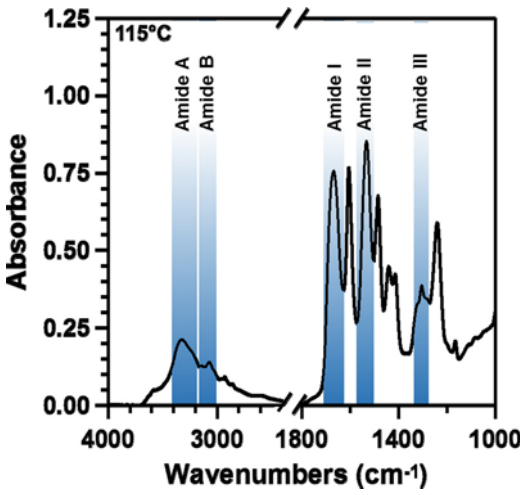

FIG. 9. (Color online) FTIR absorbance spectrum of polyamide MLD film grown on ZrO_2 nanoparticle substrate using 25 MLD cycles at 115 °C and 20 RPM with Cv = 0.017 for both TMC and mPD. Characteristic positions of amide absorption bands are shown for comparison.

C=O stretch of carboxylic acid functionalities at 1710–1800 cm^{-1}. The absence of these vibrational features in Fig. 9 suggests that TMC fully reacts with the mPD precursor during MLD film growth.

To test the thermal stability of the polyamide film, FTIR spectra of the polyamide film were monitored versus sample temperature. Figure 10 shows the infrared absorbance of the polyamide film after heating to 350, 400, 450, and 500 °C under a constant flow of 1.0 Torr UHP N_2. For reactor temperatures up to 375 °C, little change was observed in the infrared absorbance spectrum. These results are in good agreement with studies of other aromatic polyamides that are typically stable to at least 400 °C.[45–47]

At temperatures >400 °C, the infrared absorbance from the amide A and amide B bands attributed to N-H stretching vibration in the polyamide film is rapidly lost. A similar loss is observed for the amide I–III bands. This absorbance reduction is consistent with the thermal degradation of aromatic polyamides.[45–47] The thermal degradation involves the cleavage of the aromatic –NH bond and the loss of H_2O to form aromatic nitriles.[47] The H_2O can then react with an amide linkage to produce a carboxylic acid end group and an aromatic amine.[47] CO_2 can then be produced by the decarboxylation of the carboxylic acid group.[47]

Micro Raman measurements were also performed on a 200 nm thick spatial MLD polyamide film deposited with TMC and mPD at 115 °C and 20 RPM. Peaks were observed at 1000, 1120, 1250, 1350, 1560, 1605, and 1670 cm^{-1}. Several of these peaks agree with the peaks at 998, 1330, 1588 and 1612 cm^{-1} monitored using micro Raman analysis on a polyamide film grown using liquid phase chemistry with the same TMC and mPD precursors.[48] The peak at ~1000 cm^{-1} was the strongest peak for the polyamide films grown using both liquid chemistry and MLD techniques.

The micro Raman peaks can be compared with the FTIR absorption peaks. Although the selection rules are different for Raman and infrared absorption, the vibrational origins of these peaks are similar. The observed micro-Raman peak at 1670 cm^{-1} is slightly shifted from the FTIR peak at 1665 cm^{-1} and is attributed to the C=O stretching vibrations of the amide group of the amide I band. The peak at 1250 cm^{-1} matches well with the amide III band observed in the FTIR spectrum. The peak at 1560 cm^{-1} agrees fairly well with the amide II band from in plane N-H and C-N stretching vibrations as monitored in the FTIR spectrum at 1530 cm^{-1}. The peak at 1605 cm^{-1} agrees well with the peak observed in the FTIR spectrum at 1610 cm^{-1}. This peak is attributed to C=C vibrational stretching within the aromatic ring structures.

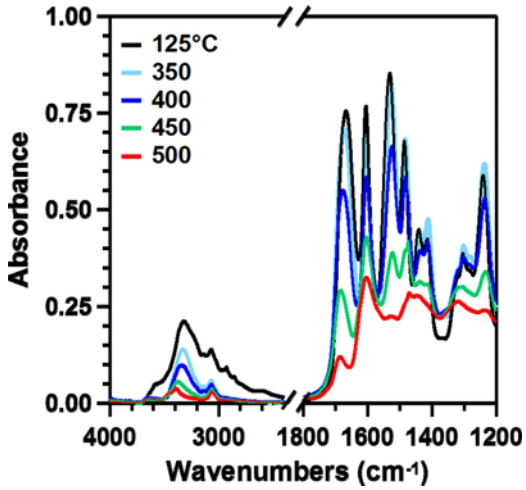

FIG. 10. (Color online) FTIR absorbance spectrum of polyamide MLD film after heating to 350, 400, 450, and 500 °C under constant flow of 1.0 Torr UHP N_2.

XPS analysis was also performed on ten random polyamide samples. The average atomic percentages for these ten samples were 74% C, 8.9% N, 13.6 O %, and 0.18% Cl. The detection limit for the XPS analysis was ~0.1%. The atomic percent values do not add up exactly to 100% because each of the atomic percent values is an average from ten different samples. The very low chlorine content suggests a nearly complete reaction of each TMC precursor. These XPS results are in good agreement with the results from the FTIR studies.

D. Spatial versus temporal MLD

Spatial MLD has many advantages relative to temporal MLD.[17] In temporal MLD, the organic precursors have to fill the reactor that typically has a volume of 0.5–2.0 l. This precursor filling can be time-consuming depending on the vapor pressure of the precursor. In addition, the precursor also has to be evacuated from the reactor prior to the next precursor exposure. This process can also be time-consuming, especially if there are any cold locations in the reactor.

In contrast, the precursors are only required to fill a very small reactor volume during spatial MLD. The volume in spatial MLD is the volume defined by the gap between the precursor source and the moving substrate.[25] For the experiments in this study, the gap is only 750 l m. The effective reactor volume under one precursor slit is ~1.00 cm^3 defined by the dimensions 750 l m × 8.1 mm × 165 mm. This reactor volume can coat a web material that is 165 mm wide at a speed up to ~210 m/min.

Spatial MLD can also be performed in a configuration with the pump directly pumping on the precursor as illustrated in Fig. 3. The pump can draw the precursor into the gap region before capturing the precursors in the pump. The precursors encounter the substrate in a small low conductance gap region before they efficiently move to the pump. This geometry maximizes precursor interaction with the substrate.

Spatial MLD is also expected to enlarge the number of polymers that can be grown using MLD techniques.[2,5] The efficient delivery and removal of precursors from the gap region will lead to the use of many additional precursors that have low vapor pressures and would be very difficult to employ in temporal MLD. In addition, the rapid deposition rates for spatial MLD will also enable the deposition of ~10 l m of MLD film in ~50 min based on a deposition rate of ~1900 Å/min at 210 RPM with four MLD cycles per rotation of the rotating cylinder. These rapid deposition rates will lead to many new applications of spatial MLD.

For commercialization of MLD, spatial MLD is also amenable to R2R processing.[18,20] The flexible foil can unwind from the initial roller, move under the gas source suppling the continuous flow of precursors, and then rewind on the final roller. R2R web speeds of 210 m/min are obtainable based on the current rotating cylinder reactor. This web speed is faster than web speeds of 1–100 m/min used in many R2R processes.

IV. CONCLUSIONS

Polyamide thin films were grown on flexible metalized PET substrates by spatial MLD in a rotating cylinder reactor with sequential exposures of TMC and mPD. The spatial MLD was facilitated by housing the rotating cylinder reactor in an isothermal oven enclosure at 115 °C. The reactor was configured to perform one polyamide MLD cycle for every rotation of the cylinder. Polyamide growth rates of 4.5 Å/cycle or 90 Å/min were measured at 20 RPM and a substrate speed of 0.33 m/s. Growth rates of 2.27 Å/cycle or 477 Å/min were obtained at higher rotation speeds of 210 RPM at substrate speeds of 3.5 m/s. With four MLD cycles per rotation of the rotating cylinder, spatial MLD should be able to obtain polymer growth rates of >1900 Å/min at a rotation speed of 210 RPM. These growth rates are dramatically larger than the MLD growth rates that can be obtained using temporal MLD reactors.

The thickness of the polyamide MLD film was very uniform across the metalized PET substrate. The polyamide MLD surface chemistry also displayed self-limiting behavior. Measurements of the polyamide growth rate per cycle versus TMC or mPD exposures revealed constant growth rates at larger TMC or mPD exposure. The TMC and mPD reactions also proceed to completion because FTIR evaluation of the polyamide MLD films was consistent with negligible free carboxylic acid groups. In addition, XPS analysis revealed very small levels of chlorine. Pyrolysis of the polyamide MLD films was also in agreement with the thermal stability of aromatic polyamides. Spatial MLD offers new possibilities for MLD on large area flexible substrates with much faster rates and with a wider range of low vapor pressure precursors than is currently feasible using temporal MLD.

ACKNOWLEDGMENTS

This research was funded by the Department of Energy (No. DE-EE0005771) through a subcontract from GE Global Research. The authors acknowledge useful discussions with Hua Wang of GE Global Research and Christopher Stafford of the National Institute of Standards and Technology (NIST). The authors also thank Huaxing Sun for the XPS measurements.

[1]S. M. George, Chem. Rev. 110, 111 (2010).
[2]P. Sundberg and M. Karppinen, Beilstein J. Nanotechnol. 5, 1104 (2014).
[3]S. M. George, B. Yoon, and A. A. Dameron, Acc. Chem. Res. 42, 498 (2009).
[4]R. L. Puurunen, J. Appl. Phys. 97, 121301 (2005).
[5]H. Zhou and S. F. Bent, J. Vac. Sci. Technol., A 31, 040801 (2013).
[6]Y. Du and S. M. George, J. Phys. Chem. C 111, 8509 (2007).
[7]N. M. Adamczyk, A. A. Dameron, and S. M. George, Langmuir 24, 2081 (2008).
[8]M. Putkonen, J. Harjuoja, T. Sajavaara, and L. Niinisto, J. Mater. Chem. 17, 664 (2007).
[9]A. Kim, M. A. Filler, S. Kim, and S. F. Bent, J. Am. Chem. Soc. 127, 6123 (2005).
[10]J. S. Lee, Y. J. Lee, E. L. Tae, Y. S. Park, and K. B. Yoon, Science 301, 818 (2003).
[11]A. A. Dameron, D. Seghete, B. B. Burton, S. D. Davidson, A. S. Cavanagh, J. A. Bertrand, and S. M. George, Chem. Mater. 20, 3315 (2008).
[12]B. Yoon, J. L. O'Patchen, D. Seghete, A. S. Cavanagh, and S. M. George, Chem. Vap. Deposition 15, 112 (2009).
[13]Q. Peng, B. Gong, R. M. VanGundy, and G. N. Parsons, Chem. Mater. 21, 820 (2009).
[14]B. H. Lee, V. R. Anderson, and S. M. George, Chem. Vap. Deposition 19, 204 (2013).
[15]A. I. Abdulagatov, R. A. Hall, J. L. Sutherland, B. H. Lee, A. S. Cavanagh, and S. M. George, Chem. Mater. 24, 2854 (2012).
[16]B. H. Lee, V. R. Anderson, and S. M. George, ACS Appl. Mater. Interfaces 6, 16880 (2014).
[17]P. Poodt, D. C. Cameron, E. Dickey, S. M. George, V. Kuznetsov, G. N. Parsons, F. Roozeboom, G. Sundaram, and A. Vermeer, J. Vac. Sci. Technol., A 30, 010802 (2012).
[18]E. Dickey and W. A. Barrow, J. Vac. Sci. Technol., A 30, 021502 (2012).
[19]P. S. Maydannik, T. O. Kaariainen, and D. C. Cameron, Chem. Eng. J. 171, 345 (2011).
[20]P. S. Maydannik, T. O. Kääriäinen, K. Lahtinen, and D. C. Cameron, J. Vac. Sci. Technol., A 32, 051603 (2014).
[21]P. F. Carcia, R. S. McLean, M. H. Reilly, M. D. Groner, and S. M. George, Appl. Phys. Lett. 89, 031915 (2006).
[22]M. D. Groner, S. M. George, R. S. McLean, and P. F. Carcia, Appl. Phys. Lett. 88, 051907 (2006).
[23]Y. S. Jung, A. S. Cavanagh, A. C. Dillon, M. D. Groner, S. M. George, and S. H. Lee, J. Electrochem. Soc. 157, A75 (2010).
[24]Y. S. Jung, A. S. Cavanagh, L. A. Riley, S. H. Kang, A. C. Dillon, M. D. Groner, S. M. George, and S. H. Lee, Adv. Mater. 22, 2172 (2010).
[25]K. Sharma, R. A. Hall, and S. M. George, J. Vac. Sci. Technol., A 33, 01a132 (2015).
[26]K. Sharma, D. Routkevitch, N. Varaksa, and S. M. George, J. Vac. Sci. Technol., A 34, 01a146 (2016).
[27]A. Illiberi, F. Roozeboom, and P. Poodt, ACS Appl. Mater. Interfaces 4, 268 (2012).
[28]D. H. Levy, S. F. Nelson, and D. Freeman, J. Disp. Technol. 5, 484 (2009).
[29]P. Poodt, A. Lankhorst, F. Roozeboom, K. Spee, D. Maas, and A. Vermeer, Adv. Mater. 22, 3564 (2010).
[30]A. S. Yersak, Y. C. Lee, J. A. Spencer, and M. D. Groner, J. Vac. Sci. Technol., A 32, 01a130 (2014).
[31]M. Elimelech and W. A. Phillip, Science 333, 712 (2011).
[32]K. P. Lee, T. C. Arnot, and D. Mattia, J. Membr. Sci. 370, 1 (2011).
[33]G. Y. Chai and W. B. Krantz, J. Membr. Sci. 93, 175 (1994).
[34]A. K. Ghosh, B. H. Jeong, X. F. Huang, and E. M. V. Hoek, J. Membr. Sci. 311, 34 (2008).
[35]I. J. Roh, A. R. Greenberg, and V. P. Khare, Desalination 191, 279 (2006).
[36]J. E. Gu *et al.*, Adv. Mater. 25, 4778 (2013).
[37]P. M. Johnson, J. Yoon, J. Y. Kelly, J. A. Howarter, and C. M. Stafford, J. Polym. Sci., Part B 50, 168 (2012).
[38]J. W. DuMont and S. M. George, J. Phys. Chem. C 119, 14603 (2015).
[39]T. H. Ballinger, J. C. S. Wong, and J. T. Yates, Langmuir 8, 1676 (1992).
[40]Q. Peng, K. Efimenko, J. Genzer, and G. N. Parsons, Langmuir 28, 10464 (2012).
[41]P. Poodt, J. van Lieshout, A. Illiberi, R. Knaapen, F. Roozeboom, and A. van Asten, J. Vac. Sci. Technol., A 31, 01a108 (2013).
[42]A. Ettori, E. Gaudichet-Maurin, J. C. Schrotter, P. Aimar, and C. Causserand, J. Membr. Sci. 375, 220 (2011).
[43]Y. Jin and Z. H. Su, J. Membr. Sci. 330, 175 (2009).
[44]G. D. Kang, C. J. Gao, W. D. Chen, X. M. Jie, Y. M. Cao, and Q. Yuan, J. Membr. Sci. 300, 165 (2007).
[45]X. Y. Chen and X. F. Cai, J. Therm. Anal. Calorim. 125, 313 (2016).
[46]S. H. Yang, P. Fu, M. Y. Liu, Y. D. Wang, Z. P. Li, and Q. X. Zhao, Express Polym. Lett. 4, 346 (2010).
[47]D. A. Chatfield, I. N. Einhorn, R. W. Mickelson, and J. H. Futrell, J. Polym. Sci. A 17, 1367 (1979).
[48]H. J. Kim, K. Choi, Y. Baek, D. G. Kim, J. Shim, J. Yoon, and J. C. Lee, ACS Appl. Mater. Interfaces 6, 2819 (2014).